Surface-Enhanced Raman Scattering Based Nonfluorescent Probe for Multiplex DNA Detection

ARTICLE *in* ANALYTICAL CHEMISTRY · JULY 2007

Impact Factor: 5.64 · DOI: 10.1021/ac070078z · Source: PubMed

3 AUTHORS:

Lan Sun
Edeniq Inc.
22 PUBLICATIONS **568** CITATIONS
SEE PROFILE

Chenxu Yu
Iowa State University
44 PUBLICATIONS **1,256** CITATIONS
SEE PROFILE

Joseph Irudayaraj
Purdue University
296 PUBLICATIONS **7,168** CITATIONS
SEE PROFILE

Published in final edited form as:
Anal Chem. 2007 June 1; 79(11): 3981–3988. doi:10.1021/ac070078z.

Surface-Enhanced Raman Scattering Based Nonfluorescent Probe for Multiplex DNA Detection

Lan Sun, **Chenxu Yu**, and **Joseph Irudayaraj***
Department of Agricultural and Biological Engineering and Bindley Biosciences Center (Physiological Sensing Facility), Purdue University, 225 S. University Street, West Lafayette, IN 47907

Abstract

To provide rapid and accurate detection of DNA markers in a straightforward, inexpensive and multiplex format, an alternative surface enhanced Raman scattering (SERS) based probe was designed and fabricated to covalently attach both DNA probing sequence and non-fluorescent Raman tags to the surface of gold nanoparticles (DNA-AuP-RTag). The intensity of Raman signal of the probes could be controlled through the surface coverage of the non-fluorescent Raman tags (RTags). Detection sensitivity of these probes could be optimized by fine-tuning the amount of DNA molecules and RTags on the probes. Long-term stability of the DNA-AuP-RTag probes was found to be good (over 3 months). Excellent multiplexing capability of the DNA-AuP-RTag scheme was demonstrated by simultaneous identification of up to eight probes in a mixture. Detection of hybridization of single-stranded DNA (ssDNA) to its complementary targets was successfully accomplished with a long-term goal to use non-fluorescent RTags in a Raman-based DNA microarray platform.

Keywords

DNA-AuP-RTag probes; non-fluorescent Raman tags; multiplex detection; SERS

INTRODUCTION

Among modern biosensing methodologies, direct assessment of unique DNA sequences of targeted living organisms (i.e., bacteria, viruses, etc.) offers the best specificity for identification. Rapid and accurate detection of DNA markers in a straightforward, inexpensive and high throughput format constitutes an effective and powerful screening tool that could ultimately be adapted in the early diagnosis of a variety of diseases. An efficient high throughput scheme that can screen for multiple DNA targets in parallel is highly desirable[1-3] in clinical diagnosis.

Radioactivity, fluorescence, or chemiluminescence are the most widely used labeling techniques for biological components. They all have their own strengths and weaknesses. The use of radioactive labels is becoming sparse due to safety considerations; conventional fluorescence methods are established and used widely but suffer from photobleaching and require an elaborate fabrication and analysis step when multiplexing is required. In addition, the broad emission profiles (usually 50-100 nm full-width at half-maximum (FWHM))[4, 5] of fluorophores or chemiluminescent tags lead to peak overlaps in multiplexing experiments, limiting the level of multiplexing. Novel fluorescent labels such as semi-conductor quantum

sun22@purdue.edu; yu13@purdue.edu; josephi@purdue.edu
*Email: josephi@purdue.edu; Phone: 765-494-0388; Fax: 765-496-1115

dots (QDs) have narrower spectral band (~25-40 nm FWHM) than traditional fluorophores,[6, 7] but the range of choice is limited. QDs are cytotoxic under certain conditions[8] and exhibit a blinking behavior which is disadvantageous.[9]

After the first observation of an unusually intense and enhanced Raman scattering signal of pyridine molecules adsorbed on silver electrode surfaces in 1974,[10] surface enhanced Raman scattering (SERS) technique has been developed as a promising technique for sensitive biological detection. Raman enhancement of up to 10^{14}-10^{15} could be achieved [11, 12] and single molecule detection has also been reported.[13, 14] Compared to other labels, SERS labels have a simpler and more extensive, and as yet underdeveloped labeling chemistry, sharp "fingerprint" signals (~1 nm FWHM) [5, 7] and a wide choice of labeling candidates including both fluorophores and non fluorophores,[15, 16] which provide excellent multiplexing capacity as non-photobleaching SERS labels.

Different implementation schemes of SERS labels for DNA probing have been reported. Graham et al. reported a method for detecting DNA based on the adsorption of fluorophore-labeled DNA onto colloidal silver particles which was subsequently detected by their respective surface enhanced resonance Raman scattering (SERRS) fingerprints.[17] Using the same scheme, eight commercially available fluorophores (ROX, rhodamine 6G, HEX, FAM, TET, Cy3, Cy5, TAMRA) were attached to oligonucleotide strands and were examined over a range of concentrations (~10^{-11}-10^{-7} M).[18] Cao et al. reported gold nanoparticle probes functionalized with oligonucleotides which were labeled with Raman-active dyes.[3] Wabuyele and Vo-Dingh developed a plasmonic nanoprobe composed of metal nanoparticles functionalized with a stem-loop DNA molecule tagged with a Raman label. In the absence of the target DNA, the stem-loop configuration of the probing single-stranded DNA (ssDNA) kept the Raman label in close proximity to the metal nanoparticle and produced intense SERS signals. Upon hybridization with the target ssDNA, the stem-loop configuration of the probing ssDNA was disrupted, and the Raman labels were physically separated from the metal nanoparticle, resulted in a quenching of the SERS signal.[19] SERS labeled DNA probes have been applied in bio diagnostics such as HIV detection,[4, 19] BRCA1 breast cancer gene detection,[15] and in microfluidics.[2, 20] Multiplex DNA detection using SERS labels have also been explored by Graham et al. to genotype the mutational status of the cystic fibrosis gene, regardless of whether it is a homozygote or heterozygote.[2] Six dissimilar DNA targets as well as two RNA targets with single nucleotide polymorphism were distinguished using six Raman-labeled (Cy3, TAMRA, Texas-Red, Cy3.5, Rodamine 6G, Cy5) nanoparticles by Cao et al.[3]

Most of previous SERS studies for DNA detection used commonly available fluorophores as Raman labels, and leaves the far broader range of non-fluorescent Raman tags (RTags) fairly unexplored. In this work, non-fluorescent RTags were explored for multiplexed DNA detection. The problem of obscure Raman scattering due to the displacement of fluorophores by biological media[21] was avoided. The complex chemistry to incorporate a fluorophore into a thiolated oligonucleotide[3, 19] was replaced by a simple but robust chemistry to tether DNA and non-fluorescent RTags separately onto gold nanoparticles (DNA-AuP-RTag). In a DNA-AuP-RTag probe, the probing DNA sequence is complementary to the target DNA sequence to be detected; the non-fluorescent RTag serves as a "code" for the specific probing sequence; gold nanoparticle acts as the SERS substrate. In DNA detection, Raman signal from the RTag indicates the presence of the target DNA molecule and the signal intensity could be used to quantify the target. In this work, the multiplexing capability of these novel DNA-AuP-RTag probes was tested by differentiating Raman spectra from a mixture of DNA-AuP-RTag probes. Eight different DNA-AuP-RTag probes were identified and used for direct differentiation in a mixture. Raman signals from these probes could be optimized by fine-tuning the amount of RTags used. In solution DNA hybridization was monitored using the DNA-AuP-RTag probe.

The limit of detection (LOD) and long-term stability of these DNA-AuP-RTag probes were also studied and discussed.

EXPERIMENTAL SECTION

Materials

DNA oligonucleotides with 5' thiol modification and HPLC purification were purchased from IDT (Coralville, IA). The Reductacryl was obtained from EMD Biosciences (San Diego, CA). 30 nm gold colloids were ordered from Ted Pella (Redding, CA). Tween 20, 1,2-Di(4-pyridyl) ethylene, 4-Mercaptopyridine, 2-Thiazoline-2-thiol, 3-Amino-1,2,4-triazole-5-thiol, 4,6-Dimethyl-2-pyrimidinethiol, 1H-1,2,4-Triazole-3-thiol, Pyrazinecarboxamide and 2-Thiouracil were purchased from Sigma-Aldrich (St.Louis, MO).

Reduction of Disulfide Bond

Thiolated DNA oligonucleotides obtained from IDT in a disulfide form were reduced using Dithiothreitol (DTT) immobilized onto acrylamide resin (Reductacryl) according to a protocol provided by IDT. The oligo and Reductacryl were first resuspended in water at a ratio of 1 mg oligo to 50 mg resin to ensure complete reduction and the mixture was stirred at room temperature for 15 minutes. Reductacryl was finally removed by syringe filtration (pore size 0.2 μm).

Attachment of Thiol Modified Oligos to Gold Nanoparticles

Thiol-derivated single-stranded oligonucleotide after reduction of disulfide bond was bound to 30nm gold colloids directly using the procedure developed by Demers et al. with slight modifications.[22] 2 mL of Ted Pella gold colloid (30 nm, original concentration of 0.33 nM) was centrifuged for 30 minutes at 8000 rpm (Microfuge® 18 Centrifuge, Beckman Coulter Inc., Fullerton, CA). Thiol-modified DNA oligonucleotides were added to the red oily precipitate to result in a 1 mL solution with a final oligo concentration of 1 μM. After 24 h, 110 μL of 100 mM of phosphate buffer (pH 7.4) with 0.1% Tween 20 was added to the mixture to result in a solution with a final buffer concentration of 10 mM with 0.01% Tween 20. After 30 minutes, salting was initiated slowly with 2 M NaCl until the desired salt concentration (0.1 M) was obtained. The solution was then allowed to “age” under these conditions for an additional 40 h and the excess reagents were removed by centrifugation for 30 minutes at 8000 rpm. Following the removal of the supernatant, the red oily precipitate was washed twice with 0.3 M NaCl, 0.01% Tween 20, 10 mM phosphate buffer (pH 7.4) (0.3 M PBS) by successive centrifugation and redispersion. Successful attachment was confirmed qualitatively by measuring the Raman spectra of the DNA bound to gold colloids. The amount of DNA attached was determined quantitatively by measuring the difference in absorbance at 260 nm, which is proportional to the concentration of DNA molecules in the testing range, between the original DNA solution and the supernatant collected through centrifugation using a UV-Visible spectrometer.

Attachment of Non-fluorescent RTags to Oligo Functionalized Gold Particles

1 mM solution was prepared for each of the RTags using nanopure water. For each sample, 1 mL of Raman tag solution was added to the red oily precipitate prepared from the previous step and the mixture was gently stirred for 24 h. The solution was then centrifuged for 30 min at 8000 rpm and the supernatant was removed. After washing with nanopure water, the final precipitate was redispersed in 1 mL of nanopurewater. Successful attachment could be confirmed by the fingerprint spectrum of the respective RTags.

SERS Measurement and Post-processing of the Spectral Data

Each DNA-AuP-RTag probe was evaluated individually, first to assess the key peaks and to establish a standard spectrum based on 10 replications. A series of mixture samples containing two to eight different DNA-AuP-RTag probes were tested. Four replications were measured for each mixture from different locations on the sample spot over a gold coated slide. The sample spots were dried under ambient conditions before measurement and spectra were acquired using the SENTERRA confocal Raman system (Bruker Optics Inc., Billerica, MA) with a 50X air objective (N.A. 0.75, infinity and flat field corrected). The excitation was provided by a 785 nm diode laser with 10 mW power at the laser source. A 50 μm pinhole was used for confocal imaging and the integration time for all the spectra was 20s with 3 coadditions and 3 ~ 5 cm^{-1} resolution.

All of the Raman spectra obtained were chopped to reveal Raman bands in the 400 cm^{-1} to 1800 cm^{-1} range and normalized using the Min/Max option (spectrum intensities were scaled to have an absorbance minimum of 0 and a maximum of 2) and a rubberband method (a "rubberband" like string icon stretched between the spectrum endpoints to provide the spectrum minima) was applied for baseline correction. All these manipulations were conducted using the OPUS software.

Hybridization-Melting Test in Solution Phase

500 μL of DNA1 (5'-thiol-AAA AAA AAA GCA GCC AAT TC-3', eight A spacers) functionalized gold nanoparticles were incubated with 500 μL of DNA2 (5'-thiol-AAA AAA AAG AAT TGG CTG CT-3' containing eight A spacers followed by the complementary strand) functionalized gold nanoparticles in 0.3 M PBS for 18 h at room temperature to form a binary network of gold nanoparticles via hybridization. Heat was then applied to increase the solution temperature from 25 °C to 90 °C to induce melting of the DNA complexes. UV-visible spectral characteristics of the mixture were monitored in the visible region at the points of initial mixing, after hybridization, and after melting. The same experiment was performed using DNA1-AuP-RTag-1 probe and DNA2 functionalized gold nanoparticles. For comparison, UV-visible spectra in the visible region were obtained at 25 °C and 90 °C for DNA functionalized gold particles and DNA1-AuP-RTag-1.

RESULTS AND DISCUSSION

Fabrication and Characterization of DNA-AuP-RTag Probes

The design of a DNA-AuP-RTag probe is schematically illustrated in Figure 1 where the probing ssDNA molecules and RTags are directly attached to the surface of gold nanoparticles via chemisorption. The covalently-bound RTags in close distance (nm range) to the gold surface assure strong SERS signals to be observed. Most of the RTags (Figure 2) have a thiol group, which reacts directly with gold. 1,2-Di(4-pyridyl)ethylene interacts chemically with gold colloids via the N atoms.[23] Adsorption of pyrazinecarboxamide onto a metal surface occurs via the carboxamide moiety with prior dissociation of one of the amidic hydrogen atoms.[24] The attachment of probing ssDNA molecules to gold nanoparticles was confirmed qualitatively via the SERS signal from the bound ssDNA molecules. Figure 3 shows a comparison between ssDNA (5'-thiol- AAA AAA AAA GCA GCC AAT TC-3') bound gold nanoparticles and control which does not contain ssDNA molecules. Raman bands of adenine (733 cm^{-1}, 1316 cm^{-1} and 1571 cm^{-1}), guanine (649 cm^{-1}, 678 cm^{-1} and 1571 cm^{-1}) and cytosine (785 cm^{-1}) [25-27] could be clearly observed from the ssDNA-bound samples, none of which was observed in the control, suggesting that the binding of ssDNA to the gold nanoparticles was successful.

The maximum monolayer surface coverage of gold nanoparticles by the ssDNA molecules was estimated using an electrical double layer model by assuming the negatively charged DNA backbone as a uniformly charged cylinder.[25, 28] The electrolyte, NaCl in this study, forms a diffuse double layer, co-axial with this cylinder. Debye length (L_D), the thickness of the double layer, can be estimated by Debye-Huckel approximation presented below as,

$$L_D = \kappa^{-1} = \left(\frac{1000 e^2 N_A}{\varepsilon \varepsilon_0 k_B T} \sum_i z_i^2 M_i \right)^{-1/2} \quad (1)$$

ε is the dielectric constant of water (= 76) and ε_0 is the permittivity constant (= 8.85 $\times 10^{-12}$ $C^2J^{-1}m^{-1}$); k_B is Boltzmann constant (= 1.38 $\times 10^{-23}$ JK^{-1}); T is room temperature (= 298 K); e is the charge of electron (= 1.6 $\times$ 10^{-19} C); N_A is the Avogadro's number (= 6.02 $\times$ 10^{23}); z_i is the absolute value of valence number and M_i is the molar concentration of ith type ion (= 0.1 M).

Thus, the radius of the cylindrical space occupied by one ssDNA molecule was the Debye length plus the radius of a ssDNA molecule , which was estimated to be 0.5 nm.[29] Because the area occupied by one ssDNA molecule is very small compared to the surface area of a gold particle (<1:100), a flat surface was assumed in the immediate vicinity of attachment instead of a spherical surface for simplicity. Equation 1 yielded a theoretical value for L_D as 0.95 nm. From these data, the maximum number of bound ssDNA molecules to a single gold nanoparticle can be estimated to be 428, which corresponds to a surface coverage of 25.1 pmol/cm^2. From Equation 1 it is clear that an increase in salt concentration will result in a decrease in L_D , hence an increase in the surface coverage. Further, addition of salt will bring ssDNA molecules closer to gold nanoparticles for increased attachment by partially screening the negative charges carried by both ssDNA molecules and gold nanoparticles with ions from the salt, one of the key reasons for suspending the nanoparticle-DNA probe in a salt solution. It should also be noted that in this model the dynamics of the binding of ssDNA molecules to gold nanoparticle surface, where the repulsion between surface-bound ssDNA molecules and the incoming ssDNA molecules would affect the binding rate and surface coverage, was not taken into account. Furthermore, a loosely packed cylindrical structure was assumed instead of a tightly packed hexagonal structure, which compensates for the overestimation arising from neglecting the binding dynamics of ssDNA molecules to gold nanoparticle surface. Hence the calculation of surface coverage in this model could give an estimate close to the true value.

The surface coverage of ssDNA molecules on gold nanoparticles was also determined experimentally. The average coverage was calculated to be 12.5 ± 4.9 pmol/cm^2 from an average of six replications, assuming no loss of gold particles. When the loss of gold particles during the whole process was considered (25% from an average of three replications), the surface coverage was corrected to be 16.7 ± 6.6 pmol/cm^2 assuming no DNA loss. The actual surface coverage should be between these two values and it was below the calculated theoretical surface coverage maximum. Thus, it is reasonable to believe that a monolayer of ssDNA molecule was formed on the gold nanoparticle surfaces and there is enough space for subsequent attachment of RTags to the particle surface.

After the attachment of RTags to DNA functionalized gold particles, Raman spectra were measured for the DNA-AuP-RTag probes (Figure 4) and the major Raman fingerprints observed are summarized in Table 1. Due to scaling of the figure, some of the major peaks may not be as distinct.

One of the unique characteristics of DNA-AuP-RTag probes is that RTags are not incorporated in the probing ssDNA, but rather directly linked to gold nanoparticles via strong covalent bonds. Hence the complex manipulation of probing ssDNA is avoided and the resulting probe is robust. Also the number of RTags on each gold nanoparticle is no longer limited by the

number of ssDNA molecules. The DNA-AuP-RTag probes can be designed to contain a higher number of RTags to achieve stronger signals should the application warrant. To demonstrate the feasibility of signal control, a set of probes fabricated from fixed concentration (1 μM) of ssDNA and increasing concentration of 4-mercaptopyridine (RTag-1) ranging from 1 μm to 1 mM in steps of 10X were tested. Variation of the peak intensity at 1089 cm^{-1} versus concentration of RTag-1 was shown in Figure 5. It is clear that the Raman intensity increased with an increase in the concentration of RTag-1 until a saturated surface coverage of the tag on gold nanoparticles was attained. Concentration ratio between ssDNA molecules and RTag could be optimized to achieve optimal Raman signal. Thus, it is possible to reach detection sensitivity levels close to fluorescent dye labeled DNA probes where the concentration of the fluorescent dye equals the concentration of probing DNA molecules (assuming one fluorophore per DNA molecule), limiting the detection sensitivity.

Multiplex Detection with the DNA-AuP-RTag Probes

One of the most significant advantages of Raman labels is the capability of multiplex coding for rapid identification of multiple targets without complex data processing. Two to eight DNA-AuP-RTag probes were tested (all with equal molar concentration) simultaneously, and individual probes could be easily differentiated based on their specific Raman fingerprints. Figure 6 shows the outcome of mixtures containing two (Mixture-1: DNA-AuP-RTag-1 & 2), four (Mixture-2: DNA-AuP-RTag-1, 2, 3 & 4) and eight (Mixture-3: DNA-AuP-RTag-1 to 8) probes. The number in parenthesis beside each peak label denotes the probe from which the peak originated. Due to scaling of the figure, some of the major peaks may not be as prominent as they were in the original spectra. Raman bands observed in each of the tested mixtures were listed in Table 2. According to the Raman bands, determination of identities of these RTags in these mixtures could easily be made. Since the identification is based on multiple characteristic Raman bands for most of the RTags and these Raman bands were reproducible, the accuracy is guaranteed.

Raman bands observed from the mixture samples can be attributed to vibrational modes of individual RTag molecules. Take 4-mercaptopyridine (RTag-1) for example. Raman band around 713 cm^{-1} is from the C-S stretching mode downshifts from 721 cm^{-1} upon adsorption of 4-Mercaptopyridine onto the gold surface via the S atom;[24, 30-33] Raman band around 813 cm^{-1} is due to the out-of-plane C-H deformation;[24, 30, 32] band around 1089 cm^{-1} is possibly from the in-plane C-H deformation;[32] band around 1204 cm^{-1} could come from the aromatic C-H in-plane bending;[33] the 1606 cm^{-1} band could be attributed to the ring stretch with protonated nitrogen.[32, 33] Similarly, Raman bands assigned to other RTags can be characterized according to their vibrational modes.[34-36] In addition, some of the Raman bands observed might be highly characteristic of the specific molecule due to vibrations of the molecule as a whole rather than group frequencies.[37]

It was noted that Raman signals from the last four probes were weaker than the first four probes. Multiplexing detection could be improved by increasing the concentration of the last four RTags during probe fabrication. A slight band shift (~4 cm^{-1}) was observed for different measuring locations on the slide, which was expected for SERS with gold nanoparticle[38] and did not affect the identification of individual probes. In all of the replications major characteristic bands of the respective RTags were consistently observed and revealed for probe differentiation.

It should be noted that only a small spectral range (400-1700 cm^{-1}) was utilized in this work. Considering the availability of hundreds of commercially available labels that have similar structure to the ones selected, several possible candidates for RTags exist. Following the scheme proposed in this work, DNA-AuP-RTag probes could be fabricated to increase the degree of multiplexing to beyond ten. If the spectral range beyond 400-1700 cm^{-1} is utilized,

and multivariate analysis is adopted to analyze the spectral signals, pushing the degree of multiplexing to higher levels would not be far fetched. A microarray platform utilizing multiplex DNA-AuP-RTag probes would have a significantly higher throughput and could be used to examine specific genome traits, for example, in alternative splice profiling of specific genes implicated to a certain disease.

In Solution DNA Hybridization-Melting Test

In DNA detection, it is essential to synthesize labeled probe sequences that can hybridize to target sequences. To demonstrate the feasibility of application of the DNA-AuP-RTag probes for target detection, in solution hybridization-melting test was conducted. When two batches of nanoparticles functionalized with complementary DNA strands (with or without RTag-1) were mixed, a binary network of gold nanoparticles would form due to hybridization.[39] A color change from red to purple, associated with hybridization,[40] was observed. Over the course of 18 h, the solution became clear and a pinkish-grey precipitate was formed. Hybridization was also indicated by a broadened red-shifted plasmon band[41, 42] revealed by the UV-visible spectra in the visible region (Figure 7A & B). When the temperature was increased gradually from 25 °C to 90 °C, the DNA duplexes underwent a dissociation process whereby ssDNA were formed and the color of the solution changed back to a reddish tint with the blue-shift of the plasmon band to its initial position (Figure 7A & B). To demonstrate the broadening and shift in the plasmon band originating from hybridization instead of temperature change, two control samples were tested, one of which contained gold nanoparticles functionalized with ssDNA molecules and the other contained the DNA1-AuP-RTag-1 probe. No color change or aggregation was observed in the control samples. UV-visible spectra did not show a significant difference at different temperatures (Figure 7C & D). We could thus conclude that the proposed DNA-AuP-RTag probes can hybridize with their counterpart and could be used for detection purposes. Array-format multiplexed detection experiments are in progress in the authors' lab.

Sensitivity and Long-term Stability of the DNA-AuP-RTag Probes

In an independent quantitative sensitivity study of 4-Mercaptopyridine, 2-Thiazoline-2-thiol, 4,6-Dimethyl-2-pyrimidinethiol and 1,2-Di(4-pyridyl)ethylene, RTag samples with decreasing concentrations in the range between 1 mM and 1 pM in steps of 10X were attached to gold nanoparticles in the absence of DNA molecules and Raman signals were obtained. Results show a detectable signal for concentration in the order of 10^{-7} M, which was the concentration before chemi-adsorption of the RTags to the metal surface. This should however not be construed as the detection limit. A longer integration time or a higher laser power could improve the sensitivity. The authors would like to point out that since sensitivity was not the focus of this work, further experiments on the detection limit of RTags were not pursued. In fact, a permissible higher concentration of RTags that do not affect the activity of DNA should be preferred for DNA detection. In addition, no linear relationship was observed between the Raman intensity and the concentration of Raman tags as described in the literature.[18, 21] One reason might be due to the dried form of samples used in Raman measurement, since the SERS intensity depends on the aggregation of gold particles, which may not be uniform in a dried sample.

To the best of our knowledge, this is the first report on the use of multiple non-fluorescent RTags in DNA probes. Thus, the long-term stability of these RTags was also examined. Raman spectra of the DNA-AuP-RTag probes collected after three months of storage in a refrigerator showed that neither a shift in the major Raman peaks nor a significant change in Raman intensity was observed for this duration (Figure 8). This study indicates that the chosen non-fluorescent RTags are durable and are stable during the tested time period. Long-term stability could be an important attribute during handling and storage.

CONCLUSION

A methodology to design, fabricate, and characterize DNA-AuP-RTag probes using non-fluorescent RTags was reported in this work. For the first time we have demonstrated a high degree of multiplexing (up to eight) using the DNA-AuP-RTag probes. A reasonable surface coverage of ssDNA to this probe complex was obtained so that detection of complementary targets in solution is possible. Probes fabricated with all eight nonfluorescent RTags were found to be stable over three months. The LOD of the DNA-AuP-RTag probes was not restricted by the amount of immobilized ssDNA to gold nanoparticles because both the probing DNA molecules and RTags were directly chemisorbed onto gold particles. Thus, detection sensitivity could be improved by optimizing the amount of DNA molecules and RTags. A wide range of commercially available chemicals could be chosen as potential candidates to fabricate DNA-AuP-RTag probes and the multiplexing capacity of the DNA-AuP-RTag scheme can be further increased.

ACKNOWLEDGMENT

Funding from NIH (Award No. 1 R03 CA121347-01), Oncological Sciences Center and the Center for Food Safety Engineering (Purdue University) is acknowledged.

REFERENCES

1. Han M, Gao X, Su JZ, Nie S. Nat Biotech 2001;19:631–635.
2. Graham D, Mallinder BJ, Whitcombe D, Watson ND, Smith WE. Analytical Chemistry 2002;74:1069–1074. [PubMed: 11924965]
3. Cao YC, Jin R, Mirkin CA. Science 2002;297:1536–1540. [PubMed: 12202825]
4. Isola NR, Stokes DL, Vo-Dinh T. Analytical Chemistry 1998;70:1352–1356. [PubMed: 9553492]
5. Ni J, Lipert RJ, Dawson GB, Porter MD. Analytical Chemistry 1999;71:4903–4908. [PubMed: 10565281]
6. Zhang CY, Johnson LW. Journal of American Chemical Society 2006;128:5324–5325.
7. Mulvaney SP, Musick MD, Keating CD, Natan MJ. Langmuir 2003;19:4784–4790.
8. Derfus AM, Chan WCW, Bhatia SN. Nano Lett 2004;4:11–18.
9. Shimizu KT, Woo WK, Fisher BR, Eisler HJ, Bawendi MG. Phys. Rev. Lett 2002;89
10. Fleischmann M, Hendra PJ, McQuillan AJ. Chemical Physics Letters 1974;26:163–166.
11. Kneipp J, Kneipp H, Rice WL, Kneipp K. Analytical Chemistry 2005;77:2381–2385. [PubMed: 15828770]
12. Vo-Dinh T. Trends in Analytical Chemistry 1998;17:557–582.
13. Koo T-W, Chan S, Sun L, Su X, Zhang J, Berlin AA. Applied Spectroscopy 2004;58
14. Nie S, Emory SR. Science 1997;275:1102–1106. [PubMed: 9027306]
15. Culha M, Stokes D, Allain LR, Vo-Dinh T. Analytical Chemistry 2003;75:6196–6201. [PubMed: 14616001]
16. Munro CH, Smith WE, White PC. Analyst 1995;120:993–1003.
17. Graham D, Smith WE, Linacre AMT, Munro CH, Watson ND, White PC. Analytical Chemistry 1997;69:4703–4707.
18. Faulds K, Smith WE, Graham D. Analytical Chemistry 2004;76:412–417. [PubMed: 14719891]
19. Wabuyele MB, Vo-Dinh T. Anal. Chem 2005;77:7810–7815. [PubMed: 16316192]
20. Park T, Lee S, Seong GH, Choo J, Lee EK, Kim YS, Ji WH, Hwang SY, Gweon D-G, Lee S. Lab chip 2005;5:437–442. [PubMed: 15791342]
21. Docherty FT, Clark M, McNay G, Graham D, Smith WE. Faraday Discussions 2004;126:281–288. [PubMed: 14992413]
22. Demers LM, Mirkin CA, Mucic RC, Reynolds RA, Letsinger RL, Elghanian R, Viswanadham G. Analytical Chemistry 2000;72:5535–5541. [PubMed: 11101228]

23. McMahon JJ, Dougherty TP, Riley DJ, Babcock GT, Carter RL. Surface Science 1985;158:381–392.
24. Baldwin JA, Vlčková B, Andrews MP, Butler IS. Langmuir 1997;13:3744–3751.
25. Green M, Liu F-M, Cohen L, Köllensperger P, Cass T. Faraday Discussions 2006;132:269–280. [PubMed: 16833122]
26. Short KW, Carpenter S, Freyer JP, Mourant JR. Biophysical Journal 2005;88:4274–4288. [PubMed: 15764662]
27. Naumann D. Applied Spectroscopy Reviews 2001;36:239–298.
28. Hiemenz, PC.; Rajagopalan, R. Principles of colloid and surface chemistry. 3 ed.. Marcel Dekker; New York: 1997. p. 499-533.
29. Zhou J, Gregurick SK, Krueger S, Schwarz FP. Biophysical Journal 2006;80:544–551. [PubMed: 16258042]
30. Hu J, Zhao B, Xu W, Li B, Fan Y. Spectrochimica Acta Part A 2002;58:2827–2834.
31. Jung HS, Kim K, Kim MS. Journal of Molecular Structure 1997;407:139–147.
32. Wang Z, Rothberg LJ. J. Phys. Chem. B 2005;109:3387–3391. [PubMed: 16851369]
33. Hu J, Zhao B, Xu W, Fan Y, Li B, Ozaki Y. J. Phys. Chem. B 2002;106:6500–6506.
34. Joy VT, Srinivasan TKK. Journal of Raman Spectroscopy 2001;32:785–793.
35. Birke RL, Shi C, Zhang W, Lombardi JR. J. Phys. Chem. B 1998;102:7983–7996.
36. Dollish, FR.; Fateley, WG.; Bentley, FF. In Characteristic Raman Frequencies of Organic Compounds. John Wiley & Sons; New York: 1974. p. 284-291.
37. Mayo, DW.; Miller, FA.; Hannah, RW. In Course Notes on the Interpretation of Infrared and Raman Spectra. John Wiley & Sons; Hoboken, New Jersey: 2004. p. 1-32.
38. Pergolese B, Muniz-Miranda M, Bigotto A. J. Phys. Chem. B 2004;108:5698–5702.
39. Mucic RC, Storhoff JJ, Mirkin CA, Letsinger RL. J. Am. Chem. Soc 1998;120:12674–12675.
40. Mirkin CA, Letsinger RL, Mucic RC, Storhoff JJ. Nature 1996;382:607–609. [PubMed: 8757129]
41. Storhoff JJ, lazarides AA, Mucic RC, Mirkin CA, Letsinger RL, Schatz GC. J. Am. Chem. Soc 2000;122:4640–4650.
42. Aslan K, Luhrs CC, Perez-Luna VH. J. Phys. Chem. B 2004;108:15631–15639.

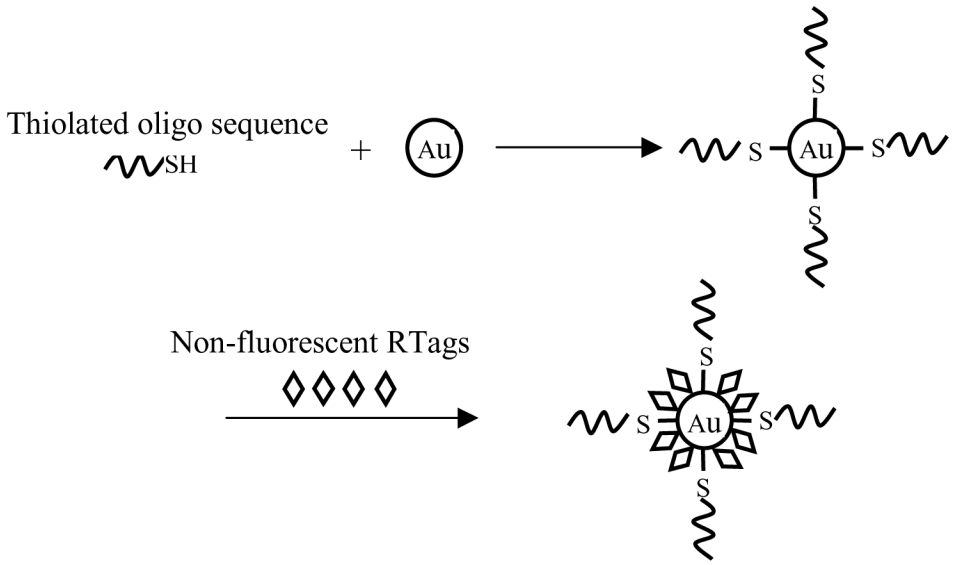

Figure 1.
Fabrication of the DNA-AuP-RTag probe.

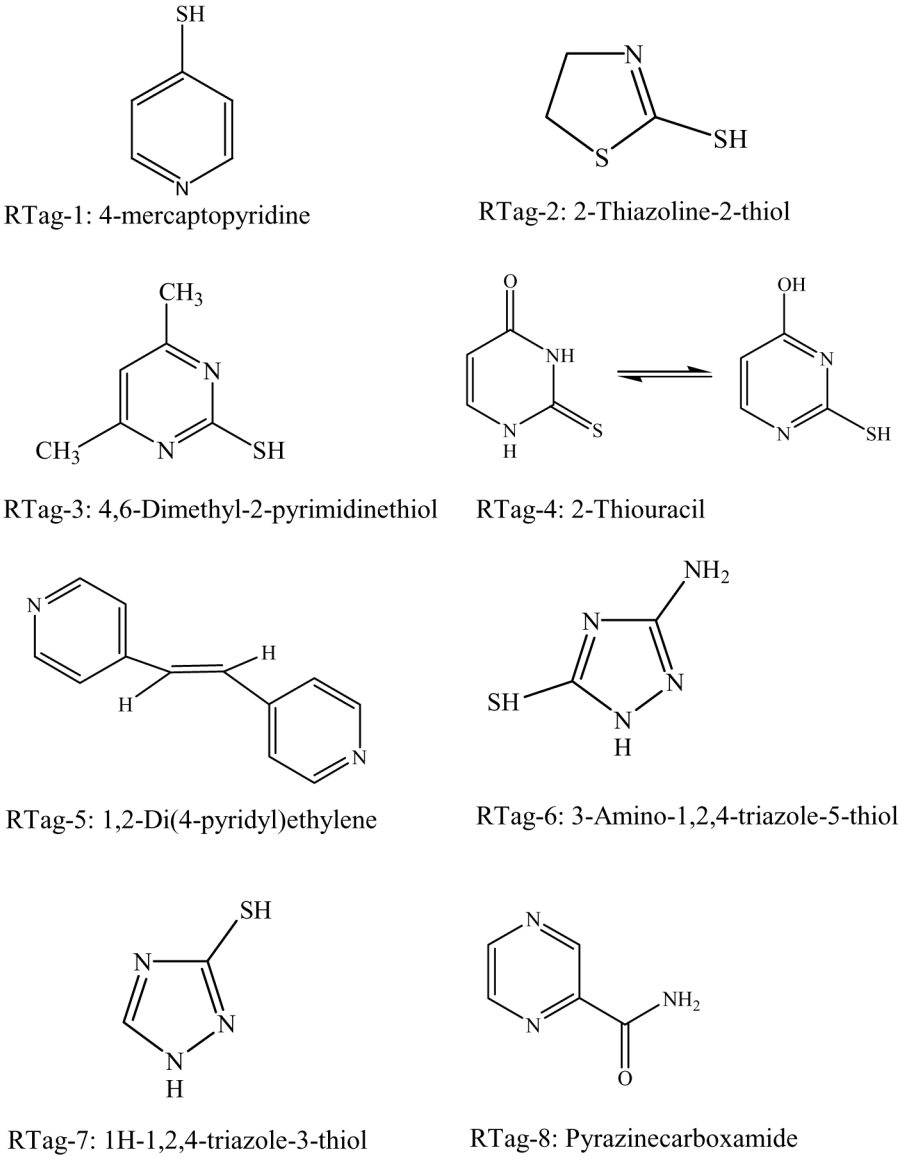

Figure 2.
Structures of selected non-fluorescent Raman tags (RTags).

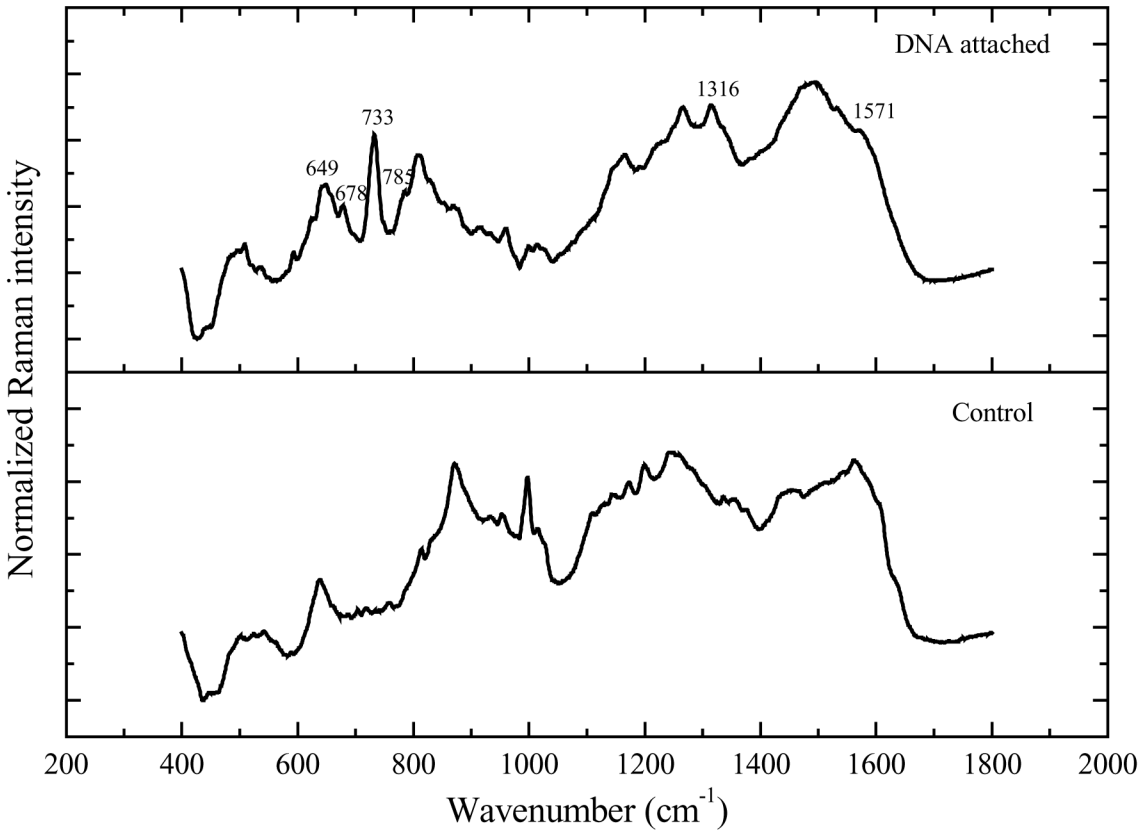

Figure 3.
Raman spectra of gold nanoparticles functionalized with 1 μM DNA (control has no DNA).

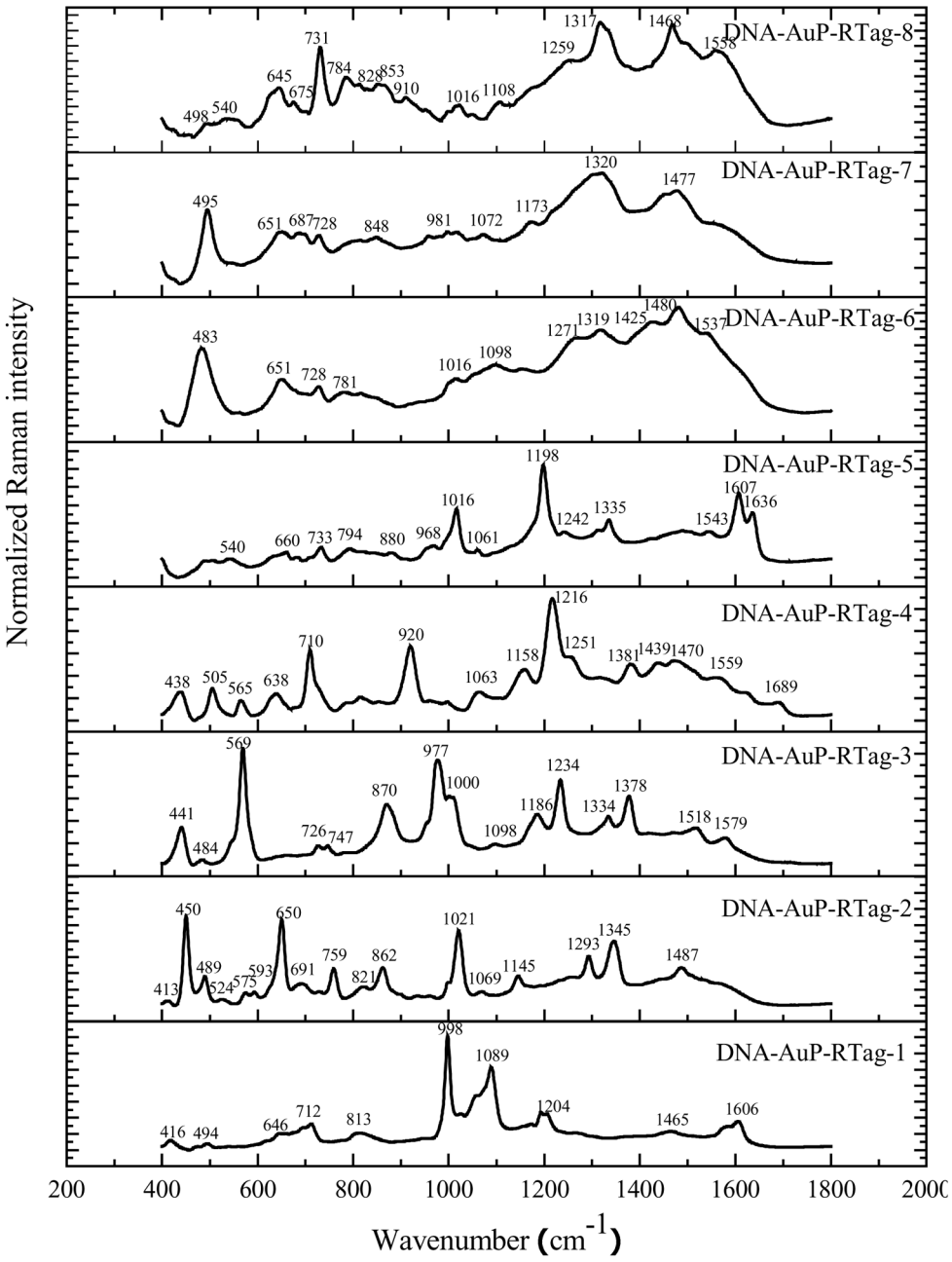

Figure 4.
Raman spectra of DNA-AuP-RTag probes.

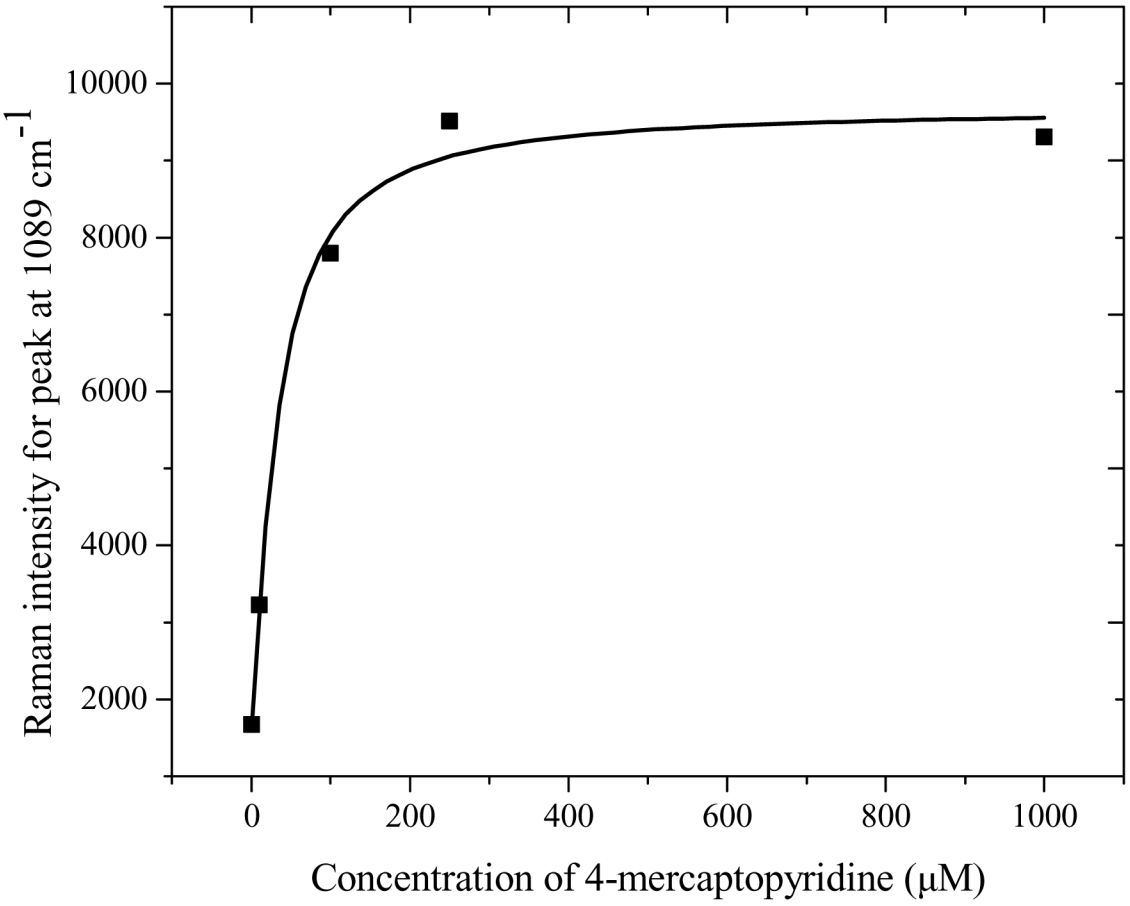

Figure 5.
Variation in Raman intensity of the peak at 1089 cm^{-1} w/r/t 4-mercaptopyridine concentration.

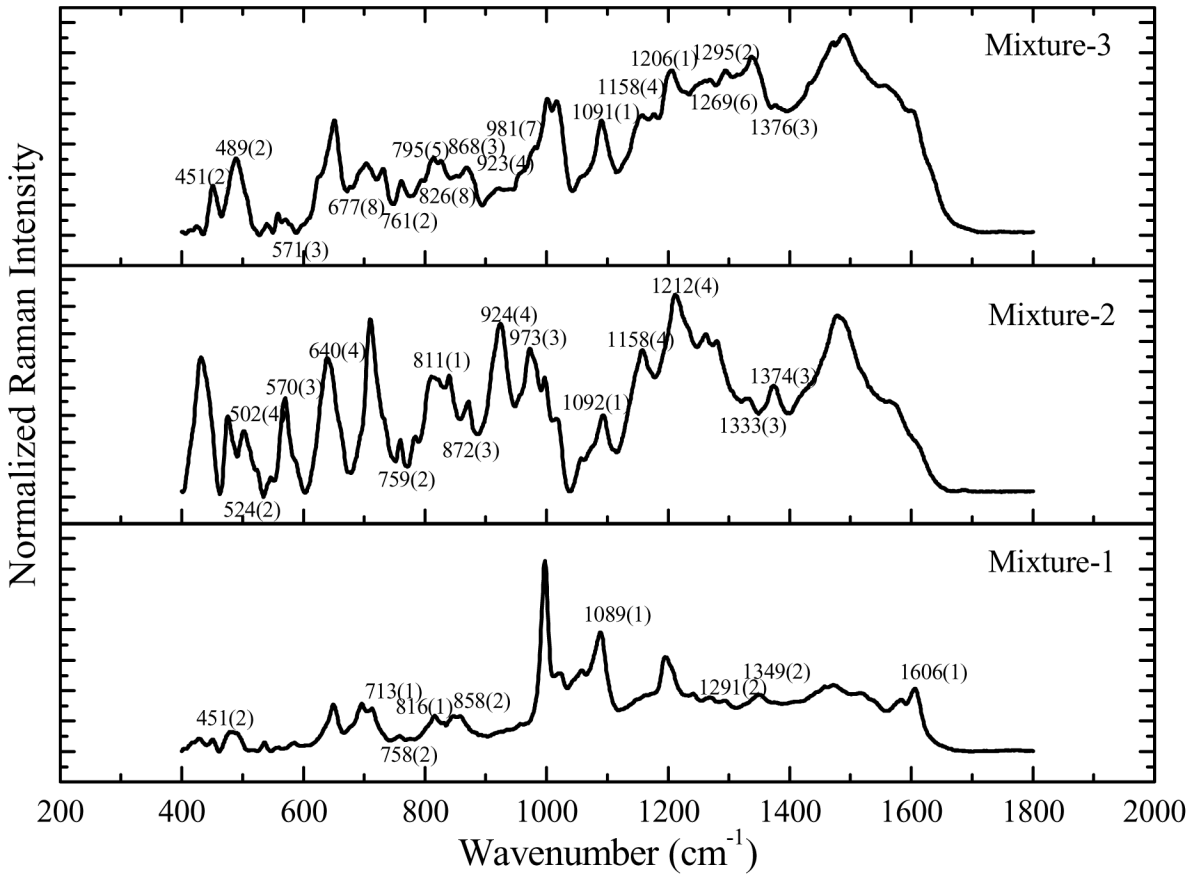

Figure 6.
Multiplex detection of DNA-AuP-RTag probe mixtures. Mixture-1: DNA-AuP-RTag-1 & 2; Mixture-2: DNA-AuP-RTag-1, 2, 3 & 4; Mixture-3: DNA-AuP-RTag-1 to 8.

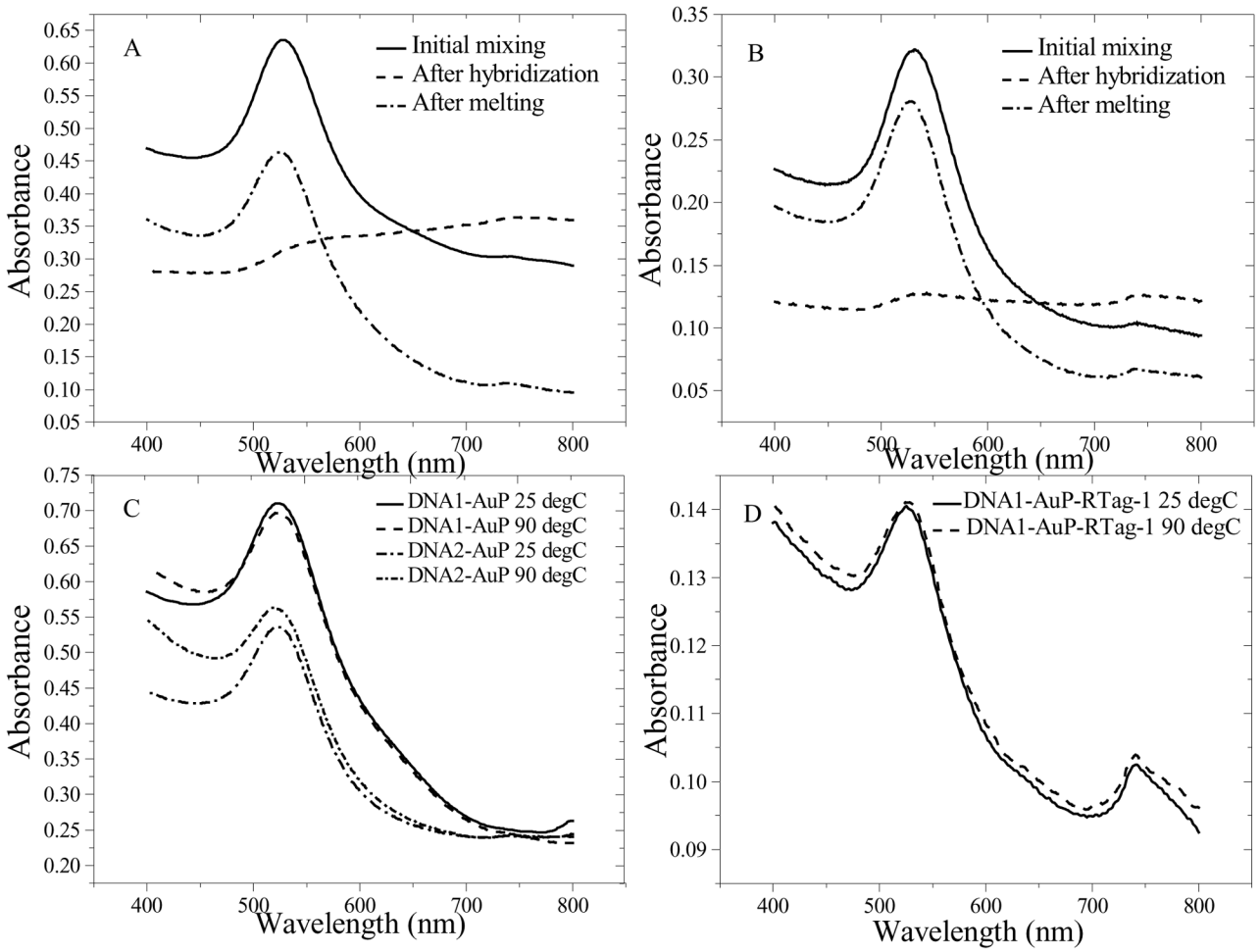

Figure 7.

Change in absorbance in the visible region of the UV-visible spectra for **(A)** mixture of DNA1 (5'-thiol-AAA AAA AAA GCA GCC AAT TC-3', eight A spacers) and DNA2 (5'-thiol-AAA AAA AAG AAT TGG CTG CT-3' containing eight A spacers followed by the complementary strand) functionalized gold nanoparticles **(B)** mixture of DNA1-AuP-RTag-1 and DNA2 functionalized gold nanoparticles **(C)** gold nanoparticles functionalized with ssDNA molecules at different temperature **(D)** the DNA1-AuP-RTag-1 probe at different temperature.

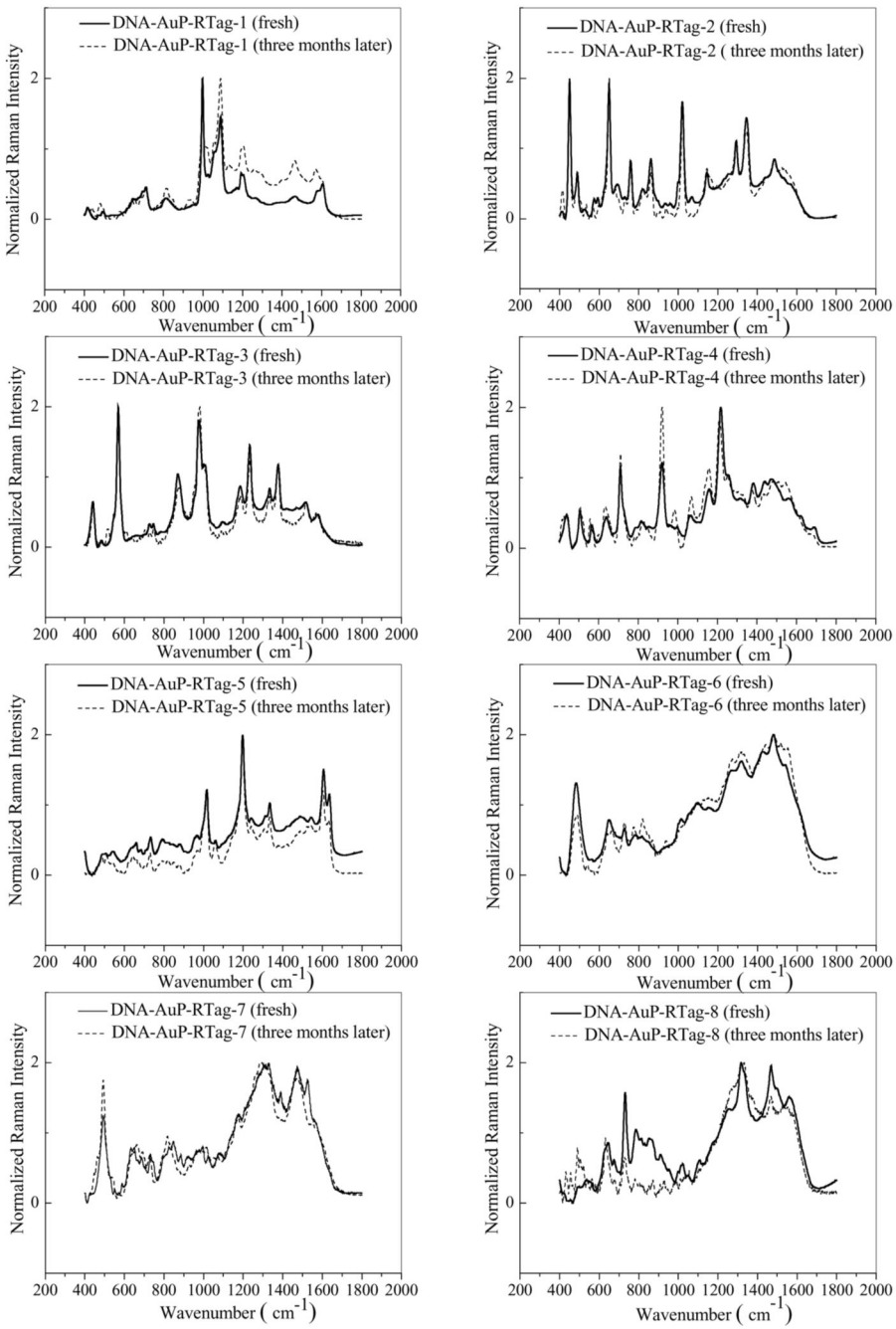

Figure 8.
Long-term stability of the DNA-AuP-RTag probes.

Table 1

Raman fingerprints observed for each of the DNA-AuP-RTag probes

Probe Name	Observed Raman Peaks (cm-1)
DNA-AuP-RTag-1	416, 494, 646, 712, 813, 998, 1089, 1204, 1465, 1606
DNA-AuP-RTag-2	413, 450, 489, 524, 575, 593, 650, 691, 759, 821, 862, 1021, 1069, 1145, 1293, 1345, 1487
DNA-AuP-RTag-3	441, 484, 569, 726, 747, 870, 977, 1000, 1098, 1186, 1234, 1334, 1378, 1518, 1579
DNA-AuP-RTag-4	438, 505, 565, 638, 710, 920, 1063, 1158, 1216, 1251, 1381, 1439, 1470, 1559, 1689
DNA-AuP-RTag-5	540, 660, 733, 794, 880, 968, 1016, 1061, 1198, 1242, 1335, 1543, 1607, 1636
DNA-AuP-RTag-6	483, 651, 728, 781, 1016, 1098, 1271, 1319, 1425, 1480, 1537
DNA-AuP-RTag-7	495, 651, 687, 728, 848, 981, 1072, 1173, 1320, 1477
DNA-AuP-RTag-8	498, 540, 645, 675, 731, 784, 828, 853, 910, 1016, 1108, 1259, 1317, 1468, 1558

Table 2

Identification of multiple DNA-AuP-RTag probes in a mixture

Sample Name	Mixture Components	Observed Raman Peaks (cm-1)
Mixture-1	DNA-AuP-RTag-1 (1) DNA-AuP-RTag-2 (2)	713, 816, 1089, 1606 451, 758, 858, 1291, 1349
Mixture-2	DNA-AuP-RTag-1 (1) DNA-AuP-RTag-2 (2) DNA-AuP-RTag-3 (3) DNA-AuP-RTag-4 (4)	811, 1092 524, 759 570, 872, 973, 1333, 1374 502, 640, 924, 1158, 1212
Mixture-3	DNA-AuP-RTag-1 (1) DNA-AuP-RTag-2 (2) DNA-AuP-RTag-3 (3) DNA-AuP-RTag-4 (4) DNA-AuP-RTag-5 (5) DNA-AuP-RTag-6 (6) DNA-AuP-RTag-7 (7) DNA-AuP-RTag-8 (8)	1091, 1206 451, 489, 761, 1295 571, 868, 1376 923, 1158 795 1269 981 677, 826